

Modern shell-model diagonalizations with realistic NN forces

C. Qi¹ and F.R. Xu^{1, 2, 3, *}

¹*School of Physics and MOE Laboratory of Heavy Ion Physics, Peking University, Beijing 100871, China*

²*Institute of Theoretical Physics, Chinese Academy of Sciences, Beijing 100080, China*

³*Center for Theoretical Nuclear Physics, National Laboratory for Heavy Ion Physics, Lanzhou 730000, China*

(Dated: May 16, 2018)

The spectral and statistical properties of nuclei ^{46}V and ^{48}Cr are studied in the framework of nuclear shell model. A microscopical effective Hamiltonian derived from the CD-Bonn NN potential is employed. The calculations are preliminary results of a newly developed parallel shell-model code. Calculations with the realistic NN interaction reproduce well the ground-state rotational band and backbending phenomenon in ^{48}Cr . A sudden alignment of all particles is seen above the backbend. The nearest-neighbour spacing distribution in ^{46}V is presented and compared with the predictions of random-matrix theory. Significant deviation from the single Gaussian-orthogonal-ensemble distribution is obtained, indicating that the isospin-symmetry breaking is not so strong in the nucleus.

PACS numbers: 21.30.Fe, 21.60.Cs, 24.60.Lz, 21.10.-k

The nuclear shell model has been considered as the most fundamental tool for the investigation of nuclear structures and electromagnetic and weak transitions. It provides the microscopic basis to study the nature of nuclear states, magnetic and quadrupole moments, β and γ transitions and nuclear reactions. The simplest version of the shell model, the so-called independent particle model, has been proposed more than fifty years ago and gives successful descriptions of the nuclear magic numbers and ground-state angular momenta with the introduction of strong spin-orbit coupling interaction [1]. Soon, the community realized the importance of introducing configuration-mixing in explaining the spectroscopic properties of nuclei (i.e., ^{19}F) with singular ground-state spins [2, 3]. The configuration-mixing concept has been considered as the essence of modern shell model calculations [4, 5, 6].

Now the shell model has been well understood in the language of perturbation theory. The basis to study the nuclear many-fermion systems is a non-relativistic Schrödinger equation which has infinite freedom and insolvable. As done in atomic many-body studies, the starting point is to reduce the Schrödinger equation to finite freedom with the help of Feshbach operators [7, 8]. The Schrödinger equation can be written in the form

$$\begin{pmatrix} PHP & PHQ \\ QHP & QHQ \end{pmatrix} \begin{pmatrix} P\Psi \\ Q\Psi \end{pmatrix} = E \begin{pmatrix} P\Psi \\ Q\Psi \end{pmatrix}, \quad (1)$$

where H is the original Hamiltonian, E the eigen energies and P and Q projection operators defining the model space and the excluded orthogonal space. From Eq. (1) we can derive an model-space dependent effective Hamiltonian which is given by [9]

$$H_{\text{eff}} = P \{ H + H \frac{1}{E - QH} QH \} P. \quad (2)$$

The original eigen energies and wave functions can be constructed by diagonalizing this equivalent Hamiltonian. The effective Hamiltonian in Eq. (2) is energy dependent and can be solved self-consistently [7] or perturbatively [8]. In the latter case the effective Hamiltonian can be written as

$$H_{\text{eff}} = PH_0P + PV\Omega P, \quad (3)$$

where H_0 is the unperturbed Hamiltonian, Ω the wave function operator and V the nuclear force. The last term is referred to as the effective residual interaction with $v_{\text{eff}} = PV\Omega P$. In the shell model context, the single particle Hamiltonian is evaluated from the experimental observations of the single particle outside the assumed core. The effective interaction v_{eff} is usually treated perturbatively up to two-body level and expressed as two-body matrix elements in harmonic oscillator (HO) basis. The shell structure of nuclear systems recognized by Mayer *et al.* [1] makes it possible to constraint calculations in one or several major shells defined by the projection operator P which can embed the dominant component of the the original wave function.

Although calculations can be restricted in a single major shell, the corresponding Hilbert space dimension is still very large. The fp shell (with M-scheme dimension around 10^9) presents the state-of-the-art shell-model performance in the past decade. Diagonalizations for nuclei in the intermediate fp model space (e.g., ^{56}Ni), however, are still painstaking [10]. Hence, the development and optimization of shell-model diagonalization algorithm has been a longstanding work [5, 10, 11, 12, 13, 14, 15, 16, 17, 18]. The first implementation of efficient shell-model diagonalization is the Oak-Ridge Rochester code [11] using the $j-j$ coupled scheme [1]. Another revolutionary development attributes to the Glasgow group [12]. The algorithm implemented by Whitehead *et al.* [12] introduced the M-scheme representation and the Lanczos diagonalization method. The M-scheme is compatible with basic bit operations in modern computer and avoids the

*Electronic address: frxu@pku.edu.cn

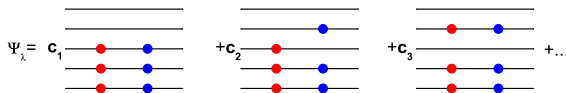


FIG. 1: Schematic picture for shell-model wave function as an expansion of partitions. The lines indicate single-particle orbits in the HO basis.

time-consuming calculations of coefficients of fractional parentage (CFP) in $j-j$ scheme. The Lanczos algorithm uses an iterative procedure and is suitable for giant matrix diagonalizations [5, 14]. The powerful shell-model code ANTOINE of the Strasbourg-Madrid group succeeded the idea of the Glasgow algorithm [14].

In M-scheme, only J_z and T_z are good quantum numbers, leading to a maximal dimension of the generated Hamiltonian matrix. The famous OXBASH code and its MSU version [13] follows a hybrid algorithm between the M-scheme and the $j-j$ coupled scheme. The symmetry of J (T) is restored through a projection procedure. The dimension of the matrix can be significantly reduced through this symmetry restoration. The algorithm implemented in OXBASH makes it very efficient to calculate many converged vectors for a given angular momentum. However, the projection process is very time-consuming and has precision problems.

In this paper we report on preliminary results calculated with a newly developed parallel shell-model code. It follows the hybrid algorithm of OXBASH and embeds a projection procedure to generate basis with good J quantum number. The program is written in Fortran 90 format which is more efficient and is more suitable for high performance computing than the outmoded FORTRAN 77 standard [19]. In Fortran 90 language, the precision of data objects can be easily defined, while super-large matrices and arrays can be handled. The code is implanted on the 64-bit Beowulf cluster of PKU computer center. Parallel algorithms are realized with the help of Message Passing Interface (MPI) [20].

The starting point of the calculation is to generate a set of bases with good magnetic quantum number in M-scheme. Neutrons and protons are blocked into two spaces. The bases are classified according to the distributions of particles in the single-particle orbits (referred to as partitions). Schematic figure for shell model wavefunction as an expansion of partitions is plotted in Fig. 1. Since the angular-momentum projection operator can only change the magnetic quantum number, projected vectors in different partitions are orthogonal, ensuring that projections can be done for each partition separately. In Fig. 2 we plotted M-scheme dimensions, $j-j$ scheme dimensions and number of partitions for 0^+ states in fp -shell $N = Z$ nuclei as a function of neutron (proton) numbers.

Vectors with good angular momentum are expanded in M-scheme bases for each partition, which can be given

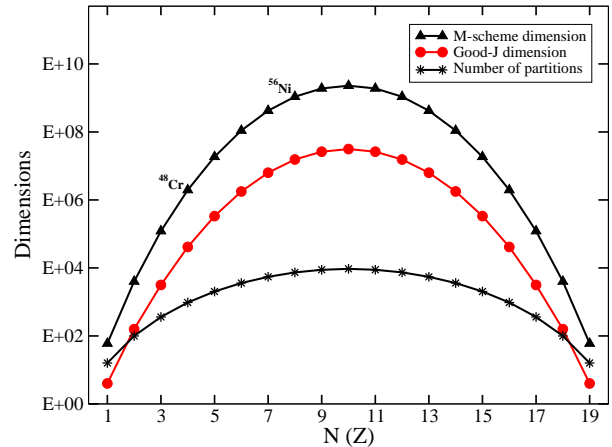


FIG. 2: M-scheme and $j-j$ coupled scheme dimensions for 0^+ states in fp shell $N=Z$ nuclei. Stars denote the numbers of partitions for each state.

as

$$|\Psi_i^J\rangle = \sum_{m \leq i} \mathcal{M}_{im} P^J |\alpha_m\rangle, \quad (4)$$

where P^J is the projection operator and $|\alpha\rangle$ a set of specially chosen M-scheme bases. \mathcal{M} is a lower triangle matrix. Vectors with good angular momentum are the orthonormal and satisfy,

$$\begin{aligned} \langle \Psi_i^J | \Psi_j^J \rangle &= \langle \Psi_i^J | \sum_{m \leq j} \mathcal{M}_{jm} P^J |\alpha_m\rangle \\ &= \sum_{m \leq j} \mathcal{M}_{jm} \langle \Psi_i^J | \alpha_m \rangle \\ &= \delta_{ij}. \end{aligned} \quad (5)$$

Elements of \mathcal{M} can be obtained by inverting the matrix $\langle \Psi_i^J | \alpha_m \rangle$. Since the projection operator satisfies, $P^J \cdot P^J = P^J$, the n -th vector can be obtained through,

$$|Q_n\rangle = |\alpha_n\rangle - \sum_{i < n} \langle O_i | \alpha_n \rangle \sum_{j \leq i} \mathcal{M}_{ij} |\alpha_j\rangle, \quad (6)$$

and

$$|\Psi_n^J\rangle = P^J |Q_n\rangle (\langle Q_n | P^J | Q_n \rangle)^{-1/2}. \quad (7)$$

In the meanwhile, matrix elements in the n -th row of the \mathcal{M} is calculated. This projection algorithm is very efficient since calculating operations and the number of coefficients needed in the calculation are comparatively small and can be stored in the computer memory. Projections for various partitions can be done independently and can run parallelly with very high scalability.

The projection procedure shown above was suggested but not used in OXBASH [13] since it does not conserve t_z values and is unsuitable for projections in isospin space. The advantages of isospin space lie in that only the smaller set of (J, T) vectors satisfying $J = J_M$ and

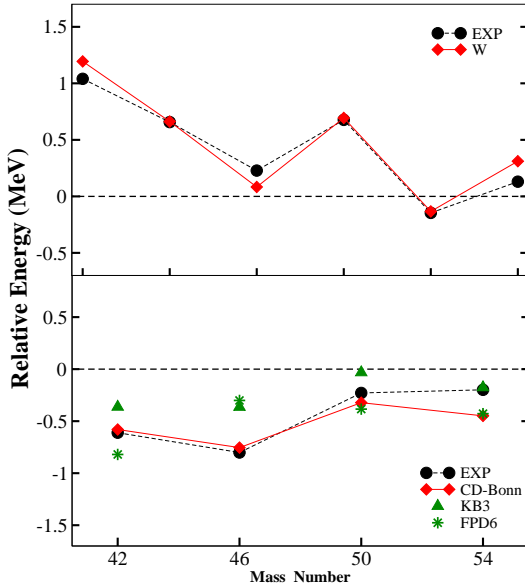


FIG. 3: Relative energies of first $T = 1$ states ($J^\pi = 0^+$) and first $T = 0$ states for odd-odd $N = Z$ nuclei ($T_z = 0$) in the sd and $0f_{7/2}$ shells. Experimental data are taken from Ref. [25]. Calculations for sd and $0f_{7/2}$ shells are done with the W [21] and CD-Bonn [26], KB3 [22] and FPD6 [23] interactions, respectively.

TABLE I: Examples of states in even-even nuclei that have $T > |T_z|$. Calculations are done using the W interaction [21].

Nuclei	J^π	Cal. (MeV)	Exp. (MeV)
^{20}Ne	1^+_1	11.20	11.26
^{24}Mg	1^+_3	9.99	9.97
^{28}Si	1^+_3	10.81	10.72
^{32}S	1^+_2	7.06	7.00
^{36}Ar	2^+_3	6.65	6.61
^{36}Ar	3^+_2	7.46	7.34
^{36}Ar	1^+_3	8.19	8.13

$T = T_z$ are projected. The number of non-zero Hamiltonian matrix elements is also smaller. The restriction of $J = J_M$ is valid since the Hamiltonian is invariant under rotations in angular momentum space. However, nuclear states with $T > T_z$ do exist and can exist at very low excitation energies. Examples in odd-odd and even-even nuclei are shown in Fig. 3 and Table I, respectively. To give the full level structure, besides the generation of the smaller (J, T) set with $T = T_z$, projections in isospin space have to be imposed to the maximum of the T value.

Since the nuclear force V is a scalar product and conserves spin and parity, the effective interaction can be simply expressed as

$$v_{\text{eff}} = \sum_{\alpha \leq \beta; \gamma \leq \delta} \langle \alpha \beta; J | V | \gamma \delta; J \rangle, \quad (8)$$

where α denotes the single-particle orbit. If isospin is

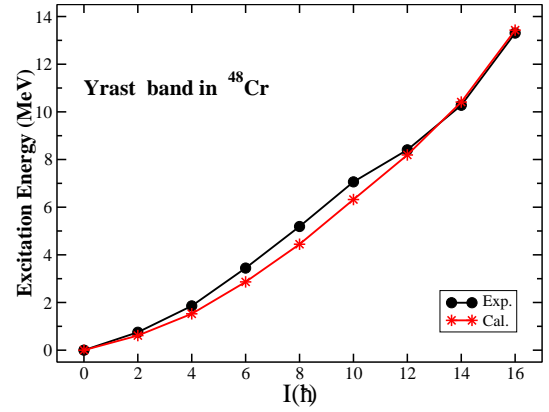


FIG. 4: Calculated and experimental yrast band in ^{48}Cr .

conserved in the Hamiltonian, the two-body matrix elements can be further simplified by adding isospin quantum numbers to the proton-proton and neutron-neutron ($T = 1$) and proton-neutron ($T = 0$ and 1) interactions, which are restricted by $J + T = \text{odd}$ for $\alpha = \beta$ and/or $\gamma = \delta$. The Hamiltonian matrix elements are given as,

$$\langle \Psi_i^J | H | \Psi_j^J \rangle = \sum_n \mathcal{M}_{jn} \langle \Psi_i^J | H | \alpha \rangle. \quad (9)$$

In practical calculations, the matrix $\langle \Psi_i^J | H | \alpha \rangle$ are calculated first and store in memory. The total matrix elements are generated by scanning and timing the \mathcal{M} matrix. The calculation of Hamiltonian matrix elements can be separated by partition and done parallelly. However, the efficiency is not optimal when dimensions are not very giant. Another very efficient way is to separate the above two steps into two or several computing processes.

The Hamiltonian matrix is diagonalized using the Lanczos procedure [5, 12]. The most time-consuming part is the iterative generating of Lanczos vectors,

$$\beta_{n+1} \rangle = H | \beta_n \rangle, \quad (10)$$

where $|\beta_0\rangle$ is a specially chosen basis in $j-j$ scheme. In the present code, the Hamiltonian matrix elements are scattered into available processes using the MPI paradigm [20], in which the matrix-array production can be done parallelly and be reduced to give out the new Lanczos vectors.

The maximum capacity of the computer code has not been tested, which can be restricted by the Input/Output operation rate of the computing system. In this work we present calculations for nuclei ^{46}V and ^{48}Cr . The largest $j-j$ scheme dimension is about 2.5×10^5 , for which the scalability of the diagonalization using up to 30 processors is still optimal.

In the past decade, the medium-mass nucleus ^{48}Cr , which has a half-filled $0f_{7/2}$ shell of protons and neutrons, has been under intensive study (see e.g. Ref. [27] and reference therein). A well-deformed ground state

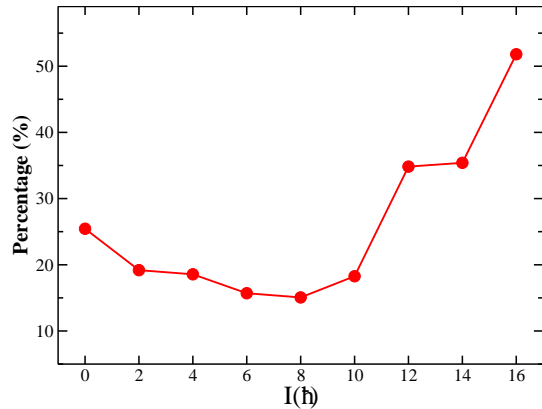


FIG. 5: The percentage of pure $0f_{7/2}^8$ configuration in the wave functions of yrast states in ^{48}Cr .

appears in ^{48}Cr , together with many macroscopic phenomena, like rotation, backbend and triaxial deformation [27, 28]. Previous shell-model study by Caurier *et al.* using a modified Kuo-Brown interaction reproduced the yrast band and the backbending phenomenon [28].

In the present work, We used an isospin-nonconserving effective Hamiltonian to study the structure of ^{48}Cr in full fp shell. The effective interaction is derived microscopically from a high-precision charge-dependent Bonn potential [26]. Single-particle energies are taken from experimental observations of odd neutron and odd proton with respect to the core of ^{40}Ca , in which the Thomas-Ehrman shift of proton $1p$ orbits can also be taken into account approximately. Excellent agreements with experiments is seen till the band terminated state with $I = 16^+$. Calculations characterize the backbend appeared at $I = 12^+$. Detailed analyse of wave functions shows that, for all states in Fig. 4, the average numbers of particles in $0f_{7/2}$ orbit (or $0f_{7/2}$ orbital occupancy) are nearly constant (around six). Above the backbend, particles are suddenly aligned, which manifest itself in that pure $0f_{7/2}$ configuration significantly increases for states with $I \geq 12$. The dispersion of configurations at low spins contributes to the deformation.

The shell model provides the most promising foundation to investigate the complexity and chaotic behavior in nuclear many-body systems, which is the best test-ground for the study of quantum chaos. Comprehensive reviews on the topic can be find, e.g., in Refs. [29, 30]. Now it is believed that the level fluctuation properties (i.e., the nearest-neighbour spacing distribution (NNS)) of quantum systems with time-reversal symmetry whose classical analogs are chaotic can well described by the Gaussian orthogonal ensemble (GOE) of random-matrix theory (RMT), whereas quantum analogs of classically integrable systems follow the Poisson statistics. Particularly interesting is the statistical properties of systems with one additional approximate symmetry. If the symmetry is exact, the NNS distribution follows the superposition of two independent GOE (2-GOE) [29]. The

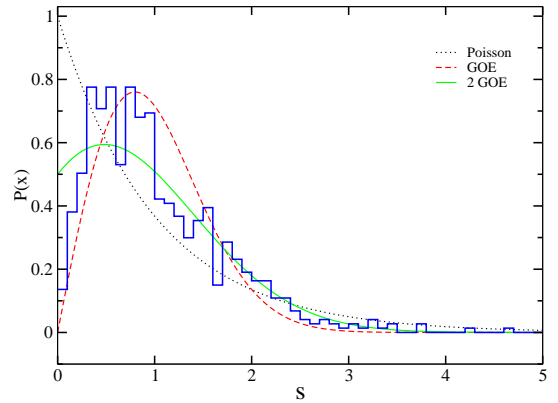


FIG. 6: The NNS distribution for low-lying levels in ^{46}V with $J < 1$.

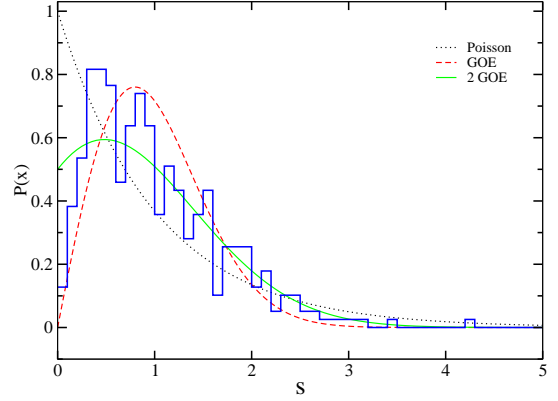


FIG. 7: Same as Fig. 6 but only for states with even spins.

complete absence of the symmetry in the distribution, however, is expected even with a small breaking of the symmetry [31]. A vivid example has been shown in the spectral statistics of acoustic resonances in rectangular quartz blocks, in which a transition from 2-GOE to GOE is seen with the gradual breaking of the point-group symmetry in the system [33].

Systematical works have been done to study the chaotic behaviors of sd -shell nuclei, both experimentally and theoretically [30]. The chaotic behavior in sd shell nuclei has been well described by shell model calculations using the empirical W interaction [21]. However, controversy still exists concerning the role played by isospin symmetry breaking on the statical properties of NNS [31]. In nucleus ^{26}Al , a system with $5p-5n$ above the core, the NNS distribution for low-lying states generated by empirical isospin-nonconserving Hamiltonian shows a strong isospin dependence, indicating that the isospin symmetry breaking is small, whereas a strong isospin symmetry breaking effect is expected from the analyse of available observations [31]. In the sd shell, strong Coulomb influence exists due to the large Thomas-Ehrman shift of proton $1s_{1/2}$ orbit. This can lead to large uncertainties [31]. One of the notable feature of the fp shell is that

the isospin symmetry breaking is relatively smaller [26]. It would be very helpful to see the statistical behavior in the shell and the isospin symmetry breaking influence. Deviation from the GOE distribution has been noticed in the NNS distribution for the low-lying states of Ca isotopes [32].

We evaluate the isospin symmetry breaking effect in the NNS distribution of ^{46}V using the isospin-nonconserving force [26] discussed above. The lowest 150 positive-parity states for each spin between $I = 0$ and 16 ($0f_{7/2}$ band termination is at $I = 15$) were calculated. The 2550 states can be generated on a single processor within an hour. The energy levels for each spin are unfolded through [32]

$$\bar{N}(E) = \int_0^E \bar{\rho}(E') dE' + N_0, \quad (11)$$

where $\bar{\rho}(E)$ is the mean level density which is assumed to be a exponential form,

$$\bar{\rho}(E) = 1/T \cdot \exp[(E - E_0)/T]. \quad (12)$$

The distribution of NNS, $P(s)$, is obtained by accumulating the number of spacings of $s_i = \bar{N}(E_{i+1}) - \bar{N}(E_i)$ within $(s, s + \Delta s)$. Results are plotted in Fig. 6 and 7.

Our calculations are carried out in proton/neutron space and is irrespective of isospin. The isospin symmetry breaking in the effective Hamiltonian has three origins: the Coulomb shifts of proton $1p$ single-particle orbits (~ 200 keV), the charge dependence in strong force and two-proton Coulomb matrix elements. If isospin symmetry is exact, the distribution should follow the 2-GOE distribution, while a transition to the single GOE

distribution is expected with the gradual breaking of isospin symmetry. Our calculations show that, however, the deviation from the 2-GOE distribution is relatively negligible. Other statistical properties, like the Brody parameter and the spectral rigidity, can provide more deep insight on this problem.

In conclusion, a new high-performance parallel shell-model code has been developed. With the code we calculated the spectral and statistical properties of nuclei ^{46}V and ^{48}Cr with a microscopical effective Hamiltonian derived from the CD-Bonn NN potential. Calculations with the realistic NN interaction reproduce well the yrast band and backbending phenomenon in ^{48}Cr . A sudden increase of pure $0f_{7/2}$ configuration is seen above the backbend. In the meanwhile, the average numbers of particles in the yrast states remains nearly constant. The NNS distribution for low-lying states in ^{46}V is calculated and compared with the predictions of random-matrix theory. The isospin-nonconserving Hamiltonian is used to evaluate the isospin symmetry breaking effect on the NNS distribution. Significant deviation from the GOE distribution is obtained, indicating that the isospin-symmetry breaking is not so strong in the nucleus.

Acknowledgement

We thank Fan Chun, Wu Zhe-ying and Pei jun-chen for useful discussions on parallel computing. This work has been supported by the Natural Science Foundations of China under Grant Nos. 10525520 and 10475002, the Key Grant Project (Grant No. 305001) of Ministry of Education of China. We also thank the PKU computer Center where the parallel code has been implanted and numerical calculations have been done.

[1] Igal Talmi, *Adv. Nucl. Phys.* **27**, 1 (2003).
[2] G. E. Tauber and Ta-You Wu, *Phys. Rev.* **93**, 295 (1954).
[3] J.P. Elliott and B.H. Flowers, *Proc. Roy. Soc.* **A229**, 536 (1955).
[4] B.A. Brown, *Prog. Part. Nucl. Phys.* **47**, 517 (2001).
[5] D.J. Dean, T. Engeland, M. Hjorth-Jensen, M.P. Kartamyshev, and E. Osnes, *Prog. Part. Nucl. Phys.* **53**, 419 (2004).
[6] E. Caurier, G. Martnez-Pinedo, F. Nowacki, A. Poves, and A.P. Zuker, *Rev. Mod. Phys.* **77**, 427 (2005).
[7] W. C. Haxton and C.-L. Song, *Phys. Rev. Lett.* **84**, 5484 (2000).
[8] I. Lindgren and J. Morrison, *Atomic Many-Body Theory* (Springer-Verlag, Berlin, 1982).
[9] C. Bloch and J. Horowitz, *Nucl. Phys.* **8**, 91 (1958); H. Feshbach, *Ann. Phys. (N.Y.)* **5**, 357 (1958).
[10] M. Horoi, B. A. Brown, T. Otsuka, M. Honma, and T. Mizusaki, *Phys. Rev. C* **73**, 061305(R) (2006).
[11] J.B. French, E.C. Halbert, J.B. McGrory, and S.S.M. Wong, *Adv. Nucl. Phys.* **3**, 193 (1969).
[12] R.R. Whitehead, A. Watt, B.J. Cole, and I. Morrison, *Adv. Nucl. Phys.* **9**, 123 (1977).
[13] A. Etchegoyen, W.D.M. Rae, N.S. Godwin, W.A. Richter, C.H. Zimmerman, B.A. Brown, W.E. Ormand, and J.S. Winfield, MSU-NSCL Report No. 524 (1985).
[14] E. Caurier and F. Nowacki, *Acta Physica Polonica* **30** (1999) 705.
[15] M. Vallieres and A. Novoselsky, *Nucl. Phys.* **A570**, 345c (1993).
[16] T. Otsuka, *Nucl. Phys.* **A704**, 21c (2002).
[17] W.E. Ormand and C.W. Johnson, *REDSTICK* code (2002).
[18] J. Toivanen, arXiv: nucl-th/0610028.
[19] A.C. Marshall, Fortran 90 Course Notes (University of Liverpool, 1997); <http://www.liv.ac.uk/HPC/>.
[20] Zhihui Du, *MPI Parallel Programming* (Tsinghua University Publication, Beijing, 2001), in Chinese.
[21] B.H. Wildenthal, *Prog. Part. Nucl. Phys.* **11**, 5 (1984).
[22] A. Poves and A.P. Zuker, *Phys. Rep.* **70**, 235 (1981).
[23] W.A. Richter, M.G. van der Merwe, R.E. Julies, and B.A. Brown, *Nucl. Phys.* **A704**, 134 (1991).
[24] M. Hjorth-Jensen, T.T.S. Kuo, and E. Osnes, *Phys. Rep.* **261**, 125 (1995); M. Hjorth-Jensen, private communication.

- [25] <http://radware.phy.ornl.gov>.
- [26] C. Qi and F.R. Xu, Int. J. Mod. Phys. **E15**, 1563 (2006); arXiv: nucl-th/0612041.
- [27] Andrius Juodagalvis, Ingemar Ragnsson, and Sven Åberg, Phys. Lett. **B477**, 66 (2000).
- [28] E. Caurier *et al.*, Phys. Rev. Lett. **75**, 2466 (1995).
- [29] Thomas Guhr, Axel Mueller-Groeling, and Hans A. Weidenmueller, Phys. Rept. **299**, 189 (1998).
- [30] V. Zelevinsky, Annu. Rev. Nucl. Part. Sci. **46**, 237 (1996).
- [31] G.E. Mitchell, E.G. Bilpuch, P.M. Endt, and J.F. Shriner, Jr., Phys. Rev. Lett. **61**, 1473 (1988); J.F. Shriner, Jr., G.E. Mitchell, and B.A. Brown, Phys. Rev. C **71**, 024313 (2005).
- [32] E. Caurier, J.M.G. Gómez, V.R. Manfredi, and L. Salasnich, Phys. Lett. **B365**, 7 (1996).
- [33] C. Ellegaard *et al.*, Phys. Rev. Lett. **77**, 4918 (1996).